LESSONS FROM A FULL SCALE FIRE TEST

B.A. Izzuddin[1] and D.B. Moore[2]

ABSTRACT

This paper draws together some important lessons from a compartment fire test conducted by BRE in the full-scale eight storey steel building at Cardington. The experiment is briefly described, and the main structural observations are highlighted. A numerical structural model of the fire compartment, using the nonlinear analysis program ADAPTIC, is then discussed. The numerical analysis employs a grillage to model the composite floor slab, and uses a one-dimensional element to model the supporting steel beams and columns. Detailed consideration of the numerical model illustrates the importance of accounting for thermal expansion effects, and leads to the identification of a load carrying mechanism at full temperature in which both the floor slab and the composite beam play an important role. A sensitivity study is then carried out in which characteristic sizes of various components and strengths of the different steel and concrete materials are varied, and the influence of such variations on the floor system response is investigated. This not only highlights the relative importance of various components in resisting the floor loading, but also sheds considerable light on the extent of plasticity developed within the various materials over the structure. Finally, several implications of the present experimental and numerical findings towards an improved design procedure, which accounts for the interaction between the floor slab and the composite beam at elevated temperature, are discussed.

[1]Reader in Computational Structural Mechanics, Dept. of Civil & Env. Eng'g, Imperial College, London.
[2]Director of Centre for Structural Engineering, Building Research Establishment, Garston, Watford.

1. INTRODUCTION

The traditional method of ensuring the strength and stability of a steel-framed structure during a fire is to cover all the exposed areas of steel with a protective material. Although this approach has proved adequate, it is extremely conservative. To address this issue research was conducted into the behaviour of isolated bare steel beams and columns which resulted in the first ever fire design code, BS5950: Part 8[1]. Similar principles were used in the development of EC3:Part 1.2[2] and EC4:Part 1.2[3]. The development of these design codes provides a more solid foundation for the provision of fire resistance to steel framed structures. However, these codes were developed from standard fire tests on isolated elements, and there is general agreement that these tests ignore the interactions that occur when elements are connected together.

In recent years, it has become increasingly clear that priority should be assigned to research to improve our understanding of the interactions between different components, leading to an appreciation of the way in which complete structural systems function when subjected to fire. Furthermore, there is a growing opinion that the structural contribution of composite steel decking flooring systems is under-utilised in current design procedures, particularly for the fire limit state. This together with investigations from real fires, such as occurred at Broadgate[4], suggests that the fire performance of complete structures is significantly better than that of the single elements from which fire resistance is universally assessed. These facts have led to a demand for full-scale fire testing.

In the early 1990's, a series of large-scale fire tests were undertaken on an eight-storey steel framed building at BRE's Cardington Laboratory. These fire tests confirmed that the performance of steel and concrete flooring systems is significantly better than that of individual steel/concrete elements. It has been suggested that this improved performance is due to the ability of lightly reinforced composite slabs to bridge over the supporting fire damaged steel

beams and to transfer their load to the undamaged parts of the steel structure.

To achieve improved understanding of the overall structural response under fire, numerical tools varying in scope and sophistication have been developed in the UK by several academic institutions, such as Imperial College[5], the University of Sheffield[6] and the University of Edinburgh[7]. This paper is concerned with modelling the corner fire test undertaken by BRE at Cardington using the Imperial College nonlinear structural analysis program ADAPTIC[8], drawing pertinent conclusions from the numerical simulation. The same test was modelled previously by Bailey[9], where shell elements were used to represent the slab which ignored geometric and material nonlinearities. This is a significant shortcoming which this paper aims to address. However, until the full development of sophisticated shell elements for composite floor slabs[10] is completed, a grillage approximation using nonlinear one-dimensional elements will be adopted for this purpose.

2. OVERVIEW OF FIRE TEST

This natural fire test was conducted within a corner compartment on the second floor of the eight-storey steel-framed building at Cardington. The size and location of the test were chosen to represent a large office room 9 m long and 6.5 m wide at the corner of the building, as shown in Figure 1, with the corresponding beam and column designations given in Table 1. The composite floor is constructed from light-weight concrete (47 N/mm^2 strength) and a PMF C70 steel deck, with a nominal A142 steel reinforcement mesh (600 N/mm^2 yield strength).

Member	***Size***	***Grade***	***Yield (N/mm^2)***
A-C, D-E	305×165UB40	43	308
F-G, A-F, C-G	356×171UB51	50	390
H-G, G-I	254×254UC89	50	390

Table 1. Sizes of steel beams and columns

In this test, described in more detail elsewhere[9], the maximum atmosphere temperature in the

centre of the compartment was 1051 °C, the maximum steel temperature recorded on the lower flange of the unprotected beam was 903 °C, and the maximum central floor displacement was of the order of 270 mm. It was clear from the test that the overall floor system maintained its structural integrity despite the very high temperature achieved in the steel beam, thus indicating a load carrying mechanism in which the floor slab plays an important role.

In view of the above, the aim of this paper is to i) establish a numerical model of the test which captures the salient response characteristics, ii) investigate the load carrying mechanism for the floor system at elevated temperature, and iii) assess through a sensitivity study the relative importance of various components in sustaining the load at elevated temperature.

3. NUMERICAL MODELLING OF FIRE COMPARTMENT

Ideally, a two-dimensional approximation is required for the floor slab. However, in the absence of realistic nonlinear shell elements for composite floor slabs[11], a grillage approximation is adopted in this study, which is considered to be realistic in terms of providing a lower bound on the structural fire resistance. It should therefore be emphasised that the main use of the adopted numerical model will be to furnish an explanation for the sustained integrity of the composite floor system at elevated temperature, instead of providing a detailed representation of all the structural, loading and response characteristics of the actual experiment.

In view of the above, the fire compartment is modelled with ADAPTIC[8] using the one-dimensional cubic beam-column formulation[12], which accounts for geometric nonlinearities[13] and for material nonlinearities using the fibre approach. Several material models can be utilised with this formulation, including the recently developed elevated temperature models for steel[5] and for concrete[14].

The compartment is considered as a substructure of the eight-storey building, where the heated floor is modelled with a lower layer of elements representing the steel beams and a top layer of

elements representing the composite floor slab with a grillage approximation, as illustrated in Figures 2 and 3.

3.1. Steel beams and columns

Steel beams A-C, D-E and F-G are each modelled with 12 elements per member, whereas beams A-F and C-G as well as columns H-G and G-I are each modelled with 10 elements per member. All connections between the steel members are assumed to be rigid, justified by the presence of a compositely acting slab in addition to compressive forces at the connections which are induced by thermal expansion effects, as considered in detail later.

The bilinear model with kinematic strain-hardening[5] is used for the steel material (Figure 4.a), where the variations of the elastic modulus (E), yield strength (σ_y) and strain-hardening parameter (μ) with temperature follow trilinear curves, as given in Table 2, and the coefficient of thermal expansion is assumed to be constant ($\alpha=1.5\times10^{-5}$ °C^{-1}).

Steel Grade	***Variation***	***E (GPa)***			***σ_y (MPa)***			***μ***		
GR43	T (°C)	0-300	600	1200	0-300	600	1200	0-200	600	1200
	Value	210	42	0	308	61.6	0	0	0.05	0
GR50	T (°C)	0-300	600	1200	0-300	600	1200	0-200	600	1200
	Value	210	42	0	390	78	0	0	0.06	0

Table 2. Material properties of steel at elevated temperature

3.2. Composite floor slab

A grillage representation is used to model the composite floor slab, where two sets of elements are employed.

The first set of elements corresponds to the part of the slab acting compositely with the steel beams, A-C, D-E and F-G. Only the solid part of the slab, with a depth of 75 mm, is considered in this respect, which is offset from the top flanges of the beams by the rib depth of

55 mm, and which incorporates a mesh of minimal steel reinforcement at 142 mm^2/m. Twelve cubic elements are used for each of the three rectangular R/C beams representing the compositely acting slab along A-C, D-E and F-G, as illustrated for the internal beam in Figure 6.b. Each of these elements are rigidly linked to the lower steel beam elements, thus implying full composite action between the slab and the beams.

The other set of elements corresponds to the part of the slab which spans in the short direction between the internal secondary beam D-E and the main beams A-C and F-G. Since the realistic modelling of this part must include the effect of the slab ribs, equivalent R/C T-beams are used along several longitudinal locations, as illustrated for an internal equivalent beam in Figure 6.c. The top-flange width of each T-beam reflects the area of the slab that the beam models, while the web width reflects an average cumulative width of the ribs, taken as 0.54m/m of top-flange width. In addition to the minimal mesh reinforcement, an equivalent steel area of 1000 mm^2/m of top-flange width is placed at 25 mm from the bottom of the slab in order to model the contribution of the steel deck. The R/C T-beams are connected to the R/C rectangular beams, whose centroidal reference line is higher, by means of rigid links which provide torsional freedom to the two sets of R/C beams. This type of connectivity, coupled with the fact that a grillage representation underestimates the in-plane shear resistance of the slab, is considered to present a lower bound on the actual slab stiffness and strength.

The same material model is used for the steel reinforcement and deck as for the steel beams (Figure 4.a), but with the material properties given in Table 3.a. For concrete, a trilinear model[14] is employed (Figure 4.b), where the variations of the maximum compressive stress (σ_c), corresponding compressive strain (ε_c) and ultimate compressive strain (ε_u) with temperature are as given in Table 3.b. The adopted concrete model ignores tensile stresses, which is consistent with common assumptions for assessing the ultimate limit state of R/C structures. Constant coefficients of thermal expansion ($\alpha=1.5\times10^{-5}$ $°C^{-1}$) and ($\alpha=0.8\times10^{-5}$ $°C^{-1}$)

are assumed for steel and concrete, respectively.

Variation	***E (GPa)***			***σ_y (MPa)***			***μ***		
T (°C)	0-300	600	1200	0-300	600	1200	0-200	600	1200
Value	210	42	0	629	126	0	0	0.05	0

Table 3.a. Material properties of floor slab mesh steel at elevated temperature

Variation	***σ_c (MPa)***			***ε_c***			***ε_u***		
T (°C)	0-300	1100	1200	0	600	900-	0	600	1200
Value	46.7	1.9	0	0.002	0.01	0.012	0.02	0.035	0.05

Table 3.b. Material properties of floor slab concrete at elevated temperature

3.3. Boundary conditions and loading

The boundary conditions applied to the substructure are as follow:

- Points A, B, C and F, are assumed to be fully restrained against all translations and rotations.
- Point G is only restrained againts vertical displacement, whereas points H and I are assumed to be fully restrained except from vertical displacement. This enables appropriate compressive forces to be applied to columns H-G and G-I, which influence the column response. Furthermore, in combination with the previous set of boundary conditions, absolute vertical support of the floor is maintained at all column positions.
- Beams A-C and A-F are restrained against transverse in-plane displacement and against rotation about the beam longitudinal axes, so as to model continuity effects imposed by the adjacent floor slab.

A uniformly distributed load of 5.48 kN/m^2 is applied to the R/C T-beams, which is transmitted to the R/C rectangular beams and from these to the steel beams through the rigid link connectors. In addition, compressive forces of 375 kN and 312 kN are applied to columns H-G and G-I, respectively, to simulate loading from the floors above.

4. PARAMETRIC INVESTIGATION OF LOAD CARRYING MECHANISM

The main purpose of this study is to investigate the possible mechanism by which the test structure sustained the applied loading at relatively high temperatures without the initiation of overall failure. Accordingly, the following simplifying approximations are made with regard to the temperature distribution over the structural components:

Steel beams A-C and F-G are heated uniformly to 700 °C.

Steel beam D-E is heated uniformly to 900 °C.

Steel beam A-F is heated uniformly to 800 °C.

Steel beam C-G is heated uniformly to 750 °C.

R/C rectangular beams are heated with a linear gradient through the depth, attaining 250 °C in the steel mesh and 100 °C at the upper surface.

R/C T-beams are heated with a linear gradient through the depth, attaining 850 °C in the reinforcement which approximates the steel deck and 250 °C in the steel mesh.

The temperatures in the various components are increased in proportion to the above values according to a common temperature factor.

To isolate the various influences of elevated temperature, consideration is given hereafter to the structural system with and without thermal expansion effects. The former case allows the influences of stiffness and strength reduction at elevated temperature to be assessed, whereas the second case is a better representation of the real system behaviour.

4.1. No thermal expansion

In order to assess the relative importance of the various structural components for this case, the coefficients of thermal expansion for all materials are taken as zero. The maximum temperatures are first applied, followed by a gradual application of the loading according to a scaling load factor, where a unit load factor corresponds to full floor loading. Three scenarios

are considered: (1) only beam D-E is heated with the rest of the structure remaining cold, (2) as before without accounting for the contribution of the steel deck, and (3) all steel beams are heated without accounting for the steel deck. Given that the steel deck is subjected to high temperatures, scenarios (2) and (3) represent a limiting condition which establishes the significance of the deck. The results for the three scenarios are shown in Figure 5.a and illustrate the importance of the steel deck in resisting the load when thermal expansion is ignored. The results also demonstrate the need to account for elevated temperatures in the compartment boundary steel beams. It is noted, however, that in the most critical scenario the central displacement at full loading is around 145 mm, which falls well short of the displacement of 270 mm observed in the test.

As a final refinement to this case, elevated temperature is considered in all components, including the beams and slab, before the loading is applied. To illustrate the validity of the attained final deformation mode under this loading scenario, the more realistic scenario involving load application before elevated temperature is also considered. In the latter case, full loading as well as a 50% increase in loading are considered prior to applying the full temperature (i.e. Temperature factor = 1). The results for the three scenarios are depicted in Figure 5.b, where it is shown that, when thermal expansion is ignored, the response is not sensitive to the order of application of loading and temperatures with regard to the final attained configuration. The predicted central displacement for the refined model subject to the full loading and elevated temperature is only 124 mm, which is over 50% less than observed in the experiment.

4.2. With thermal expansion

Thermal expansion effects are incorporated in the refined model of the previous section, where the results are shown in Figure 6.a. Three loading scenarios are again considered, and these are: (1) floor loading applied after the full temperature distribution, (2) temperature applied

after full floor loading, which closely resembles the actual loading sequence, and (3) temperature applied after a 50% increase in floor loading. The first scenario predicts an initial displacement of 175 mm due to thermal effects, which is followed by an almost linear response to subsequent loading, achieving a central displacement of 341 mm at full loading. The effective stiffness in the loading phase is smaller than the initial stiffness presented by the same loading scenario without consideration of thermal expansion effects, shown in Figure 5.b, but is greater than its final stiffness. This observation points to a kind of behaviour in the loading phase where the transition of the material response from elastic to plastic has already occurred and stabilised in most parts of the structure, and where membrane effects as well as pre-stressing of some of the concrete material due to restrained thermal expansion dominate the overall system response. The second loading scenario, which resembles more closely the actual experimental conditions, predicts a gradual degradation in stiffness, where a final displacement of 422 mm is achieved. Unlike the case ignoring thermal expansion effects, the comparison between the first two loading scenarios is not very favourable in terms of the final attained configuration, which indicates the occurrence of a considerable amount of material plasticity after the application of initial temperatures in the first loading scenario. However, it is evident that thermal expansion has a considerable influence on the response, where the predicted displacement provides an overestimate of the displacement observed experimentally by around 50%, instead of the underestimate by a similar amount presented when thermal expansion is ignored. This confirms similar observations on the importance of thermal expansion effects made by other researchers[15,16] in relation to simpler structural systems. The third loading scenario, in which the initial floor loading is increased by 50%, provides similar response characteristics to those observed in the second scenario but, as expected, achieving a larger central displacement of 508 mm.

The refined base model, considering the realistic second loading scenario, is now varied to

investigate the effects of rigid links in the slab and pinned end connections for beam D-E. As shown in Figure 6.b, the assumption of rigid links reduces the central displacement to 350 mm, which is now closer to the experimentally observed displacement of 270 mm; the 80 mm difference can be attributed to the nature of grillage approximation and to the adopted approximation of the temperature distribution. Despite the improvement achieved with rigid slab links, the base model will be adopted for detailed consideration later as an upper bound on the response, principally due to the sensitivity of the analysis based on rigid slab links to the assumed torsional rigidity in the R/C grillage beams. On the other hand, the effect of pinned end connections for beam D-E is shown in Figure 6.b to be relatively marginal, increasing the predicted displacement to 464 mm. Nevertheless, due to considerable compressive forces at the connections, as discussed in the following section, and because of composite action with the slab, the true connection behaviour is more closely approximated by the rigid assumption than the pinned one.

4.3. Load carrying mechanism

It has been shown previously that thermal expansion effects are very significant, at least with regard to the levels of displacement achieved. This section aims at investigating the mechanism by which the load is sustained at relatively high temperatures, where comparison is made between the cases ignoring and accounting for thermal expansion. Although it has been shown that the adopted base model, including thermal expansion, overestimates the observed central displacement by around 50%, this model represents an upper bound on the displacements or a lower bound on the structural resistance. Accordingly, it is anticipated that the existence of a safe load carrying mechanism under the assumptions of this model should mean that a similarly safe mechanism also exists for the real structure.

The transfer of load from the floor slab to the composite beam along D-E, that is the load transfer from the R/C T-beams to the R/C rectangular beams, is depicted in Figure 7. This

shows the averaged distributed force transferred along the composite beam D-E at ambient, intermediate and full temperatures, with and without consideration of thermal expansion effects. The results indicate that thermal expansion plays a considerable role in modifying the load carrying mechanism at intermediate and full temperatures. Without thermal expansion, the load transfer to beam D-E is reduced at full temperature, which is greater at midspan as expected. However, with thermal expansion effects, the load transfer at the edges, particularly at the inner connection, of beam D-E is considerably increased, whereas it is reduced to almost negligible levels at midspan for the full temperature. This can be explained by the presence of an additional driving force imposed by the slab on the composite beam due to thermal expansion, which is released almost completely at midspan due to the sustained deflections of the beam.

To investigate the load carrying mechanism with thermal expansion, the following parameters, i) axial force, ii) centroidal bending moment, and iii) effective eccentricity from the centroid, are examined for the internal steel beam D-E, for the R/C rectangular beam (which acts compositely with steel beam D-E), and for the inner edge as well as the central R/C T-beams. The results from the study are shown in Figures 8-11. For all components, the effective eccentricity from the centroid is taken as the ratio of the hogging centroidal bending moment to the tensile axial force. This ratio can be used to determine whether a particular cross-section is acting mainly in bending or axially.

The results in Figure 8 for steel beam D-E indicate that the response at full temperature is dominated by axial compressive behaviour at the beam ends, with the midspan region dominated by bending behaviour. Given that the effective eccentricity at the beam ends is within the cross-section boundaries, the stress state over the end cross-sections can be considered to be mostly compressive. Therefore, in the real structure, considerable rotation at the simple connections would have to overcome significant contact forces, thus justifying the

assumption of rigid connections at the beam ends.

For the compositely acting R/C rectangular beam, the results in Figure 9 indicate that the response at full temperature is dominated by tensile membrane behaviour which, from examining the effective eccentricity, is concentrated in the steel mesh reinforcement. It is worth noting that the level of tensile membrane force corresponds to stresses in the mesh which are about 40% of the yield strength, the latter not being affected by the moderate mesh temperature of 250 °C.

For the inner edge R/C T-beam, the results in Figure 10 demonstrate the considerable compressive axial forces generated, particularly at intermediate temperatures prior to degradation in the material strength. These compressive forces enable significant bending moments to be sustained by enhancing the contribution from the prestressed concrete, and are responsible for greater curvature in the bending moment diagram due to the P-Δ effect. The results indicate that the response is governed by a combination of compressive axial and bending behaviour, with the compressive forces attaining a greater value in the inner T-beam span, as would be expected. The tendency of the edge T-beam to deflect downwards, due to the thermal gradient and the restraint to thermal expansion, coupled with its greatly enhanced bending response due to compressive forces, is responsible for the considerable downwards forces that are imparted onto the composite beam D-E at the inner edge. This is illustrated in Figure 7.

Finally, for the central R/C T-beam, the results shown in Figure 11 indicate that the response at full temperature is dominated by tensile membrane behaviour, with the level of tensile force greater in the inner T-beam span, as would be expected. Under these tensile membrane forces and associated deflections, the central T-beam is capable of sustaining the distributed load almost entirely, thus transferring a negligible amount to the composite beam D-E at midspan. This is again illustrated in Figure 7.

The above observations are summarised in the diagram shown in Figure 12. This figure depicts the forces transferred from the R/C T-beams to the composite beam D-E, and the nature of the internal forces within the composite beam, for the realistic case accounting for thermal expansion effects.

4.4. Sensitivity study

The relative significance of the various structural components, with regard to the load carrying mechanism, is investigated by varying the dimensions of various components and examining the effect on the resulting deflections. Furthermore, the influence of varying the strength of steel and concrete on the deflections is also investigated. This allows the extent of the spread of plasticity within the constituent materials of the structural system to be investigated.

The sensitivity study is carried out for the case with thermal expansion, and the results are shown in Figures 13.a-b. The significance of the various components is investigated by modifying characteristic dimensions, as follows:

Steel beam D-E: Flange and web thickness

Mesh in R/C T-beams: Reinforcement area

Deck in R/C T-beams: Equivalent reinforcement area

R/C Rectangular beams: Effective width and mesh area

R/C T-beams: Top and bottom widths (only concrete area)

The strength of the various materials used is modified as follows:

GR50, GR43 and reinforcement steel: Yield strength (σ_y)

Concrete: Compressive strength (σ_c) and corresponding strain (ε_c)

The results in Figure 13.a show that the response at full temperature is most sensitive to a reduction in the concrete area of the R/C T-beam, which can be related to an increase in the load transfer to the composite beam D-E. Interestingly, a reduction in the steel deck area leads

to a reduction in the central displacement of the floor. This is in contrast to the observation in section 4.1 made for the case ignoring thermal expansion, and can be attributed to a reduction in the downwards force imparted by thermal expansion effects in the R/C T-beams. This tendency is also observed at the intermediate temperature level (Temperature factor = 0.5) when the characteristic dimensions of the steel deck as well as the R/C rectangular and T-beams are reduced. The influence of changing the material strength is shown in Figure 13.b, from which it is evident that the mesh reinforcement has the greatest effect, thus indicating that significant yielding occurs in the mesh. This yielding of the mesh is mostly in the R/C T-beams, because these span in the shorter direction. Interestingly, the deflections appear to be insensitive to the strength of concrete, indicating that concrete is far from crushing and that the overall response is consequently insensitive to the softening characteristics of the concrete material. Given that the response is shown in Figure 13.a to be very sensitive to the concrete area in the R/C T-beam, it is concluded that such sensitivity is related to the elastic response of concrete and the relative area of concrete and steel in the T-beams.

5. DESIGN IMPLICATIONS

The preceding experimental investigation demonstrated that complete steel/concrete composite flooring systems perform better in fire than isolated elements on which fire resistance is universally determined. The accompanying numerical study has provided an explanation of the sustained structural integrity at elevated temperature, which is principally related to the ability of the lightly reinforced concrete slab to bridge over the fire damaged supporting steel beam.

Under the action of increasing temperature, the numerical models have shown that a significant portion of the load is shed from the internal composite beam D-E and is taken by the composite slab in combined bending and membrane actions. The slab can conveniently be split into regions which are under pure tensile membrane action, and regions which can carry the load in bending action enhance by compressive membrane forces. The tensile membrane zone

occurs in the central region, while the enhanced bending zone occurs around the perimeter of the flooring system. This description of the flooring system behaviour suggests that the fire resistance of the system should account for the influence of thermal expansion and should include contributions from both the slab and the composite beam. The contribution that each of these components makes to the overall fire resistance of the system is discussed in more detail below, with reference to the results obtained using the realistic base model including thermal expansion effects.

5.1. Slab behaviour

The construction of a typical composite slab comprises profile metal decking which acts compositely with light-weight concrete reinforced with a nominal mesh. In practice, at the fire limit state, the profile metal decking will debond from the concrete due to the build up of steam pressure, and the decking will also be at very high temperature. Although debonding has not been considered in the numerical models, the results from the sensitivity study should still be valid at large displacements where the membrane actions in the steel decking and mesh reinforcement are more significant than the shear transfer between the decking and the concrete. While the sensitivity results indicate that reducing the steel decking area leads to a reduction in the beam deflection when accounting for thermal expansion, such a reduction is shown to be relatively small. Accordingly, it is proposed here that the steel decking can, for simplicity, be ignored in the assessment of the fire limit state for composite floor systems, provided that thermal expansion effects are accounted for.

The sensitivity study has also demonstrated that the reinforcing mesh plays an important role in determining the fire resistance of the overall flooring system. This suggests that the designer can enhance the fire performance of composite flooring systems by increasing either the area or the yield strength of the reinforcing mesh. Two parameters not considered in the current investigation are the limiting fracture strain of the mesh and the strain concentration at crack

locations. Such considerations will not affect the overall trends observed in the sensitivity study, but will simply limit the deformability of the system. This can be taken account of by adopting a pragmatic approach which either reduces the mesh strength or increases the mesh strain by a suitable safety factor. Further experimental and numerical studies are required to determine such a safety factor.

5.2. Beam behaviour

The numerical investigations have shown that the stress distribution in the composite beam is complex, varying from a compressive axial state at the connections of the steel beam to pure bending in the centre, with the reinforcement mesh in tension. Although a suitable design model based on such a stress distribution could be developed, there is no guarantee that the observed stress distribution will exist at the fire limit state. One of the benefits of thermal expansion is to induce compressive forces into the steel beam which preload the boundaries allowing them to be considered as fixed against rotation, regardless of the type of connection. From a practical point of view, the flexural behaviour of the steel beam may be modelled assuming fixed boundary conditions. Although not considered in this study, the experiments showed that the end-plate connections fractured on one side during the cooling stage due to the contraction of the steel beam which had already sustained plastic compression. The issues associated with cooling and its effect on connection behaviour should evidently be considered by the designer.

5.3. Supporting perimeter beams

As the temperature of the flooring system increases, the load carrying capacity of the inner beam D-E is decreased with the consequent shedding of the load to the slab. The slab in turn transfers more load to the perimeter beams, and these beams should be checked for this increased load at the fire limit state. These beams can be checked assuming composite action, taking account of the appropriate temperature distribution and the reduced material properties

of the steel beam and the reinforcement. Should the perimeter beams prove inadequate, the designer can improve their performance by either providing fire protection or increasing the section size.

6. CONCLUSIONS

This paper draws together some important lessons from a compartment fire test conducted by BRE in the full-scale eight storey steel building at Cardington. Following a brief overview of the experiment, a numerical model of the test using the nonlinear analysis program ADAPTIC is described.

The adopted model illustrates the importance of accounting for thermal expansion effects, and identifies a load carrying mechanism in which the floor slab plays a significant role in resisting the loading at full temperature. It is shown that tensile membrane action dominates the central region of the slab, and that bending action enhanced by compression exists along the edges of the slab, whereas the composite beam develops a rather complex stress state.

A sensitivity study is then presented, which not only highlights the relative importance of various components in resisting the floor loading, but also provides a measure of the extent of plasticity developed within the various materials. The results indicate that both the steel beam and the floor slab make significant contributions towards resisting the applied loading. Furthermore, whilst the nominal reinforcement mesh remains elastic in the long span direction, considerable yielding is sustained in the short direction. Significantly, the compressive concrete in the floor slab remains largely elastic, which has important benefits with regard to the development of simplified design procedures.

Several implications of the present experimental and numerical findings towards the fire resistance design of composite floor systems are highlighted, where it is suggested that any realistic design procedure for such systems must include the effects of restraint to thermal expansion. Furthermore, in view of the relatively small contribution from the steel deck when

accounting for thermal expansion effects, it is suggested that the deck can be ignored in fire resistance design calculations. In addition, it is proposed that the designer could achieve better control over the design of composite floor systems for fire resistance through using the mesh reinforcement area and/or strength as design parameters.

Finally, it is pointed out that, whilst failure criteria have not been considered in this work, such criteria would not change the trends observed in the sensitivity study, but would simply impose a limit on the deformability of the system. Further research is required in this area to complement the on-going research on the detailed two-dimensional modelling of composite floor slabs.

REFERENCES

1. BS5950, 'Structural use of steel in buildings: Part 8: Code of Practice for Fire Resistant Design', London, British Standards Institution, 1990.
2. Eurocode 3, 'Design of Steel Structures: Part 1.2: General Rules, Structural Fire Design', ENV 1993-1-2, Brussels, European Committee for Standardisation, 1995.
3. Eurocode 4, 'Design of Composite Steel and Concrete Structures: Part 1.2: General Rules, Structural Fire Design', ENV 1994-1-2, Brussels, European Committee for Standardisation, 1994.
4. 'Structural Fire Engineering Investigation of Broadgate, Phase 8', Ascot, Steel Construction Institute, 1991.
5. L. Song, B.A. Izzuddin, A.S. Elnashai and P.J. Dowling, 'An Integrated Adaptive Environment for Fire and Explosion Analysis of Steel Frames - Part I: Analytical Models', Journal of Constructional Steel Research, Vol. 53, pp. 63-85, 2000.
6. C.G. Bailey, I.W. Burgess and R.J. Plank, 'Computer Simulation of a Full-Scale Structural Fire Test', The Structural Engineer, Vol. 74, No. 6, pp. 93-100, 1996.
7. M. Gillie, A.S. Usmani, and J.M. Rotter, 'A Structural Analysis of the First Cardington

Test', Journal of Constructional Steel Research, Vol. 57, pp. 581-601, 2001.

8. B.A. Izzuddin, 'Nonlinear Dynamic Analysis of Framed Structures', PhD Thesis, Department of Civil Engineering, Imperial College, University of London, 1991.
9. C. Bailey, 'Computer Modelling of the Corner Compartment Fire Test on the Large-Scale Cardington Test Frame', Journal of Constructional Steel Research, Vol. 48, pp. 27-45, 1998.
10. B.A. Izzuddin, X.Y. Tao and A.Y. Elghazouli, 'Nonlinear Analysis of Composite Floor Slabs with Geometric Orthotropy', Proceedings of the Eighth International Conference on Civil and Structural Engineering Computing, Eisenstadt, Austria, 2001.
11. L. Song, 'Integrated Analysis of Steel Buildings under Fire and Explosion', PhD Thesis, Department of Civil Engineering, Imperial College, University of London, 1998.
12. B.A. Izzuddin and A.S. Elnashai, 'Adaptive Space Frame Analysis - Part II: A Distributed Plasticity Approach', Structures and Buildings, Proceedings of Institution of Civil Engineers, Vol. 99, No. 3, pp. 317-326, 1993.
13. B.A. Izzuddin and A.S. Elnashai, 'Eulerian Formulation for Large Displacement Analysis of Space Frames', Journal of Engineering Mechanics, ASCE, Vol. 119, No. 3, pp. 549-569, 1993.
14. A.J. Richardson, 'Behaviour of Composite Steel/Concrete Structures under Fire Conditions', PhD Thesis, Department of Civil and Environmental Engineering, Imperial College, University of London, (*in preparation*).
15. A.Y. Elghazouli and B.A. Izzuddin, 'Response of Idealised Composite Beam-Slab Systems under Fire Conditions', Journal of Constructional Steel Research, Vol. 56, pp. 199-224, 2000.
16. J.M. Rotter, A.M. Sanad, A.S. Usmani and M. Gillie, 'Structural Performance of Redundant Structures under Local Fires', Proceedings of Interflam 99, Eighth International

Fire Science and Engineering Conference, Edinburgh, Vol. 2, pp. 1069-1080, 1999.

FIGURE CAPTIONS

Figure 1. Structural configuration of fire compartment

Figure 2. Structural model of fire compartment

Figure 3.a. Mesh for steel beams and columns

Figure 3.b. Mesh for internal R/C rectangular beam

Figure 3.c. Mesh for internal R/C T-beam

Figure 4. Steady state stress-strain relationships

Figure 5.a. No thermal expansion: Significance of main components

Figure 5.b. No thermal expansion: Refined model

Figure 6.a. With thermal expansion: Refined model

Figure 6.b. With thermal expansion: Effect of modelling assumptions

Figure 7. Load transfer between slab and composite beam D-E

Figure 8. Axial force, bending moment and eccentricity in steel beam D-E

Figure 9. Axial force, bending moment and eccentricity in R/C rectangular beam D-E

Figure 10. Axial force, bending moment and eccentricity in inner edge R/C T-beam

Figure 11. Axial force, bending moment and eccentricity in midspan R/C T-beam

Figure 12. Composite beam D-E at full temperature

Figure 13.a. Effect of component sizes

Figure 13.b. Effect of material strength

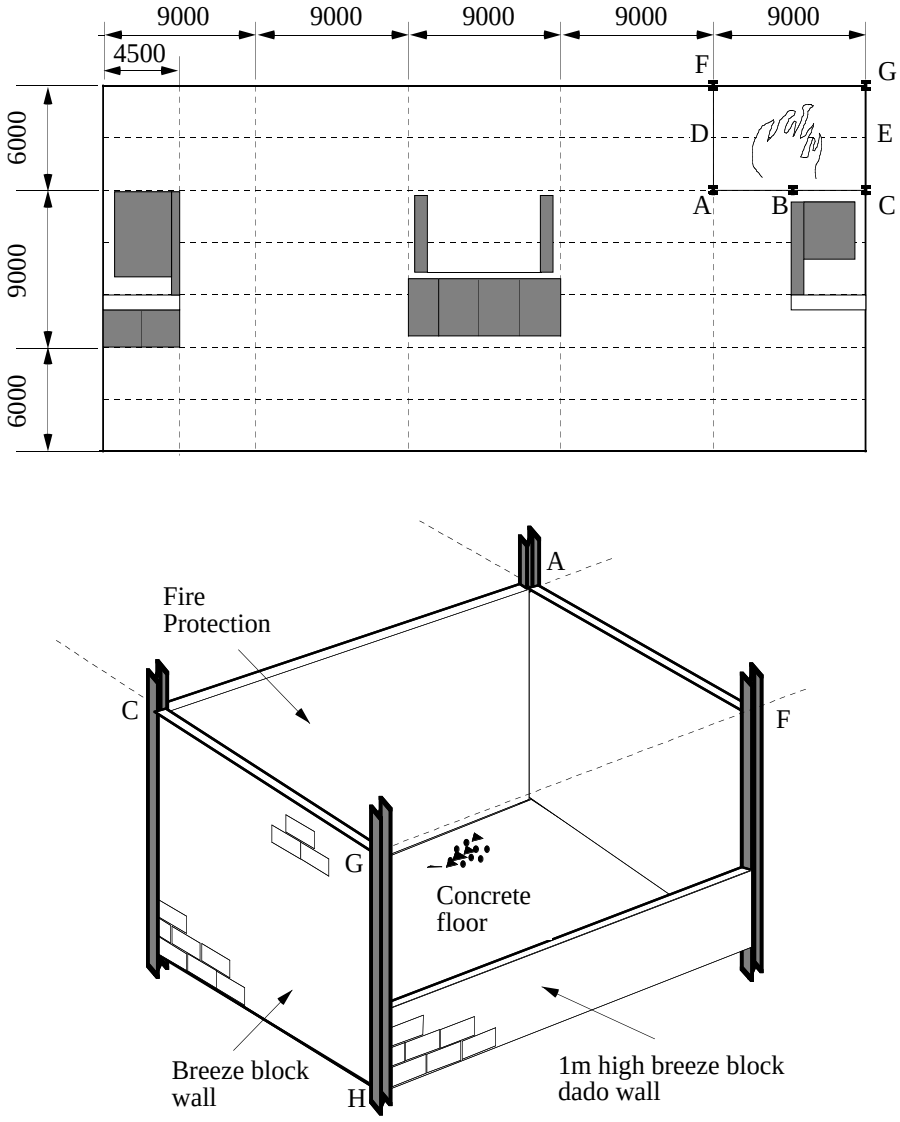

Figure 1. Structural configuration of fire compartment

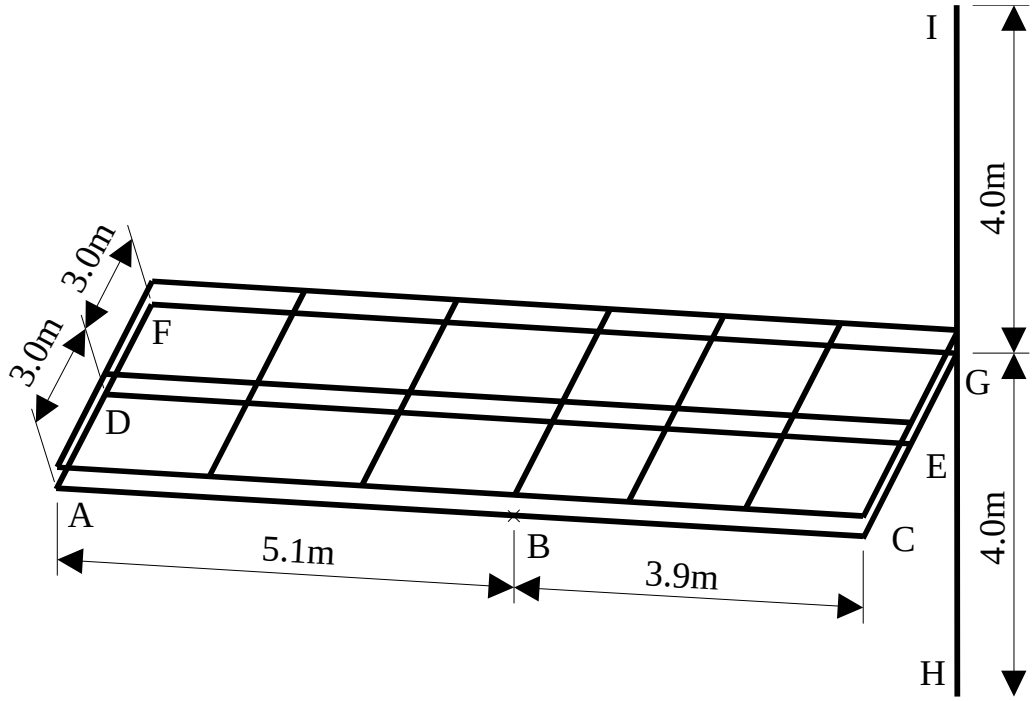

Figure 2. Structural model of fire compartment

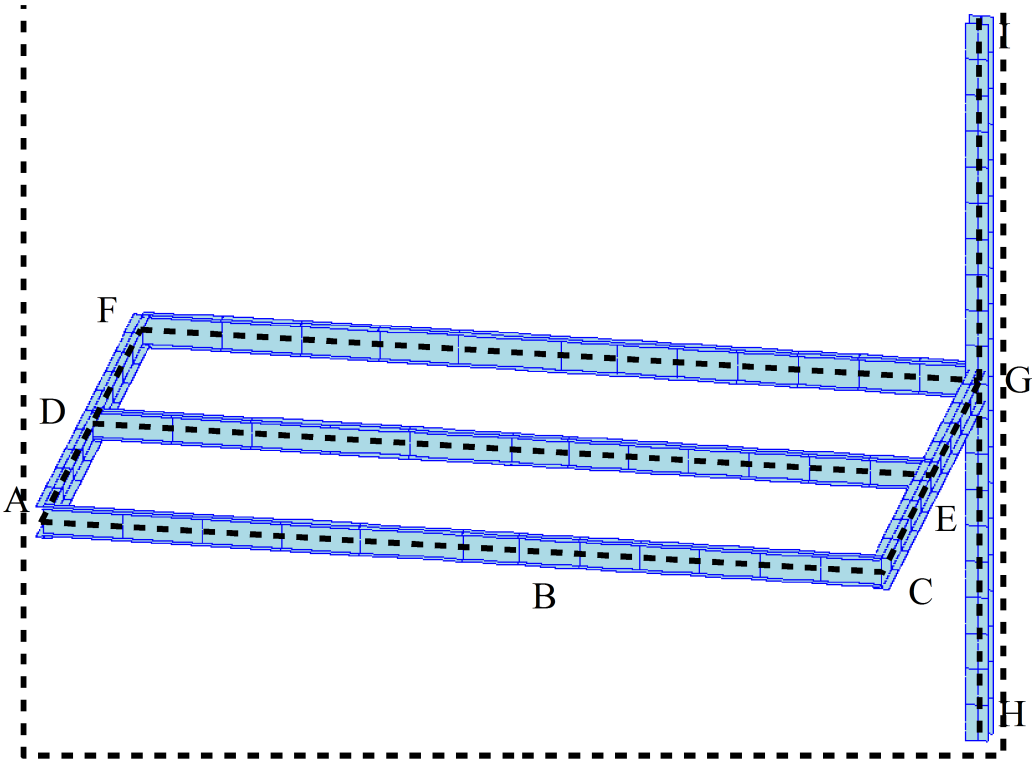

Figure 3.a. Mesh for steel beams and columns

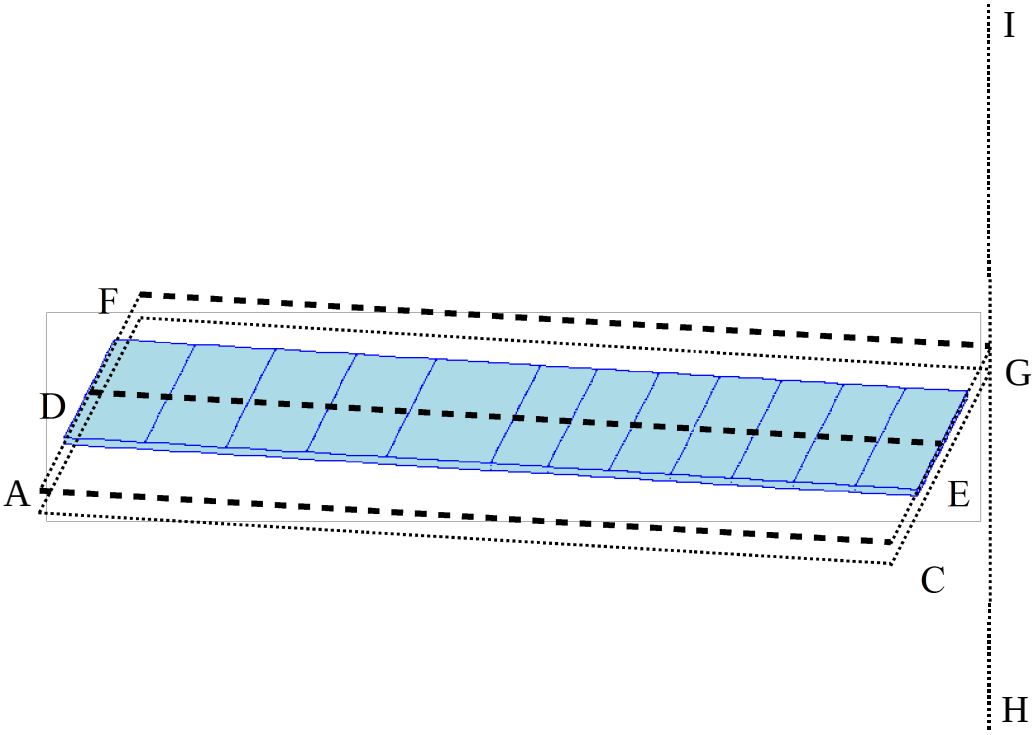

Figure 3.b. Mesh for internal R/C rectangular beam

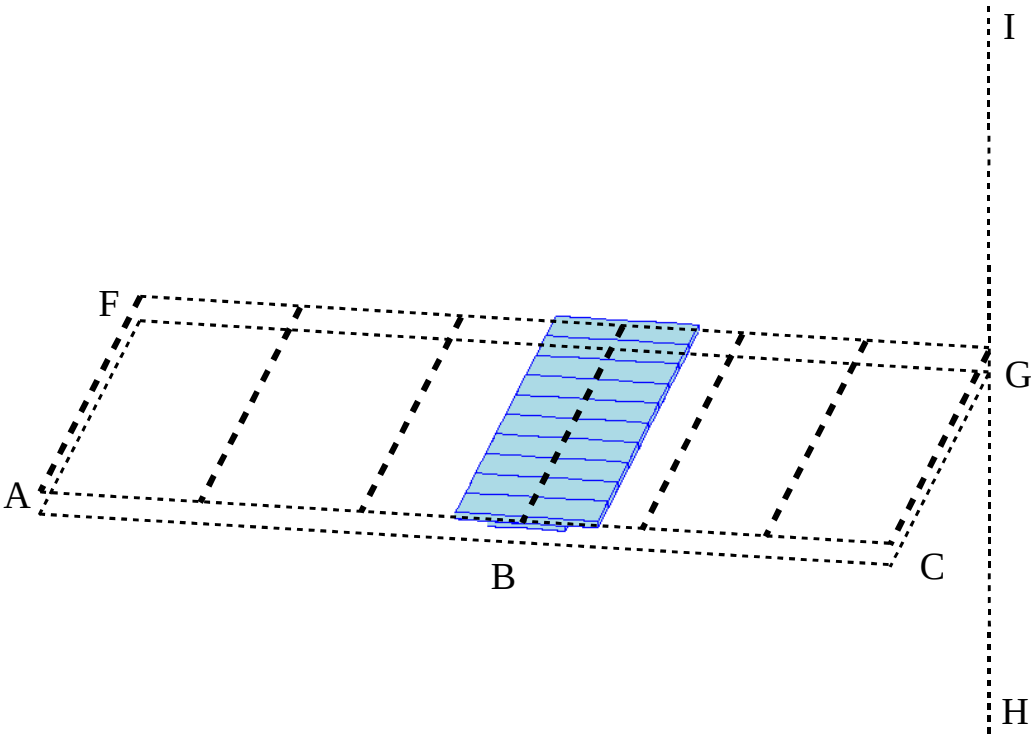

Figure 3.c. Mesh for internal R/C T-beam

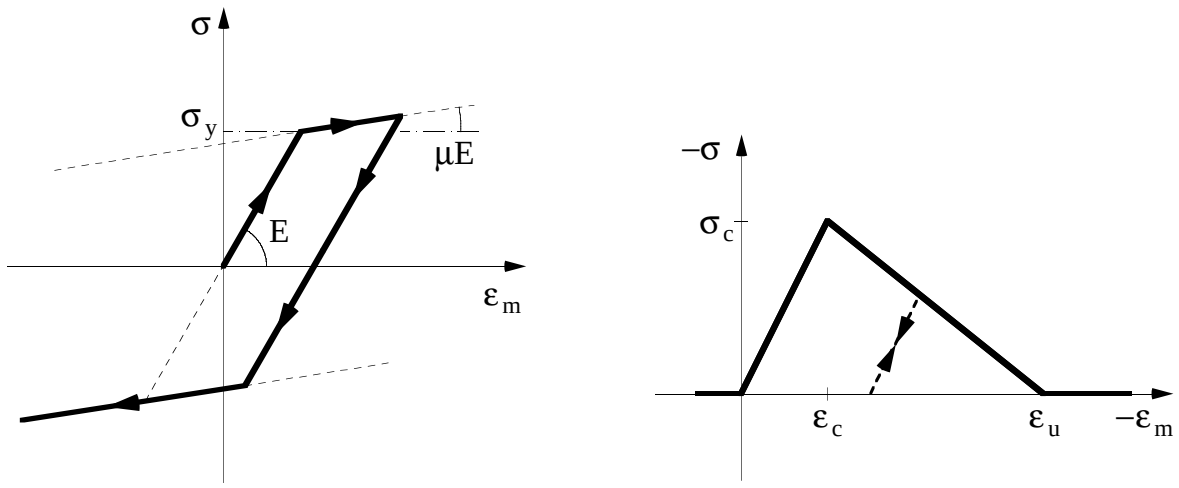

(a) Steel **(b) Concrete**

Figure 4. Steady state stress-strain relationships

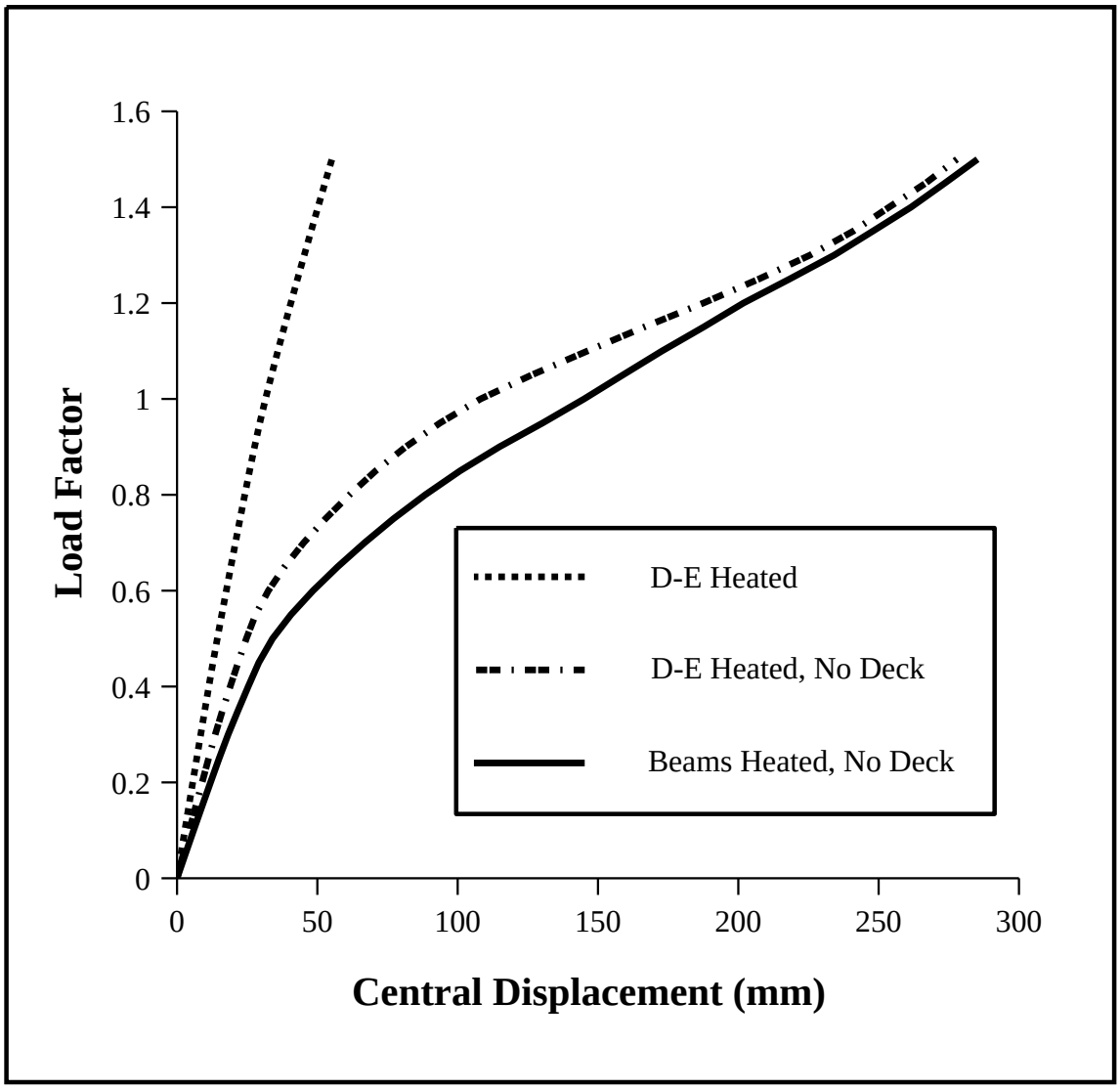

Figure 5.a. No thermal expansion: Significance of main components

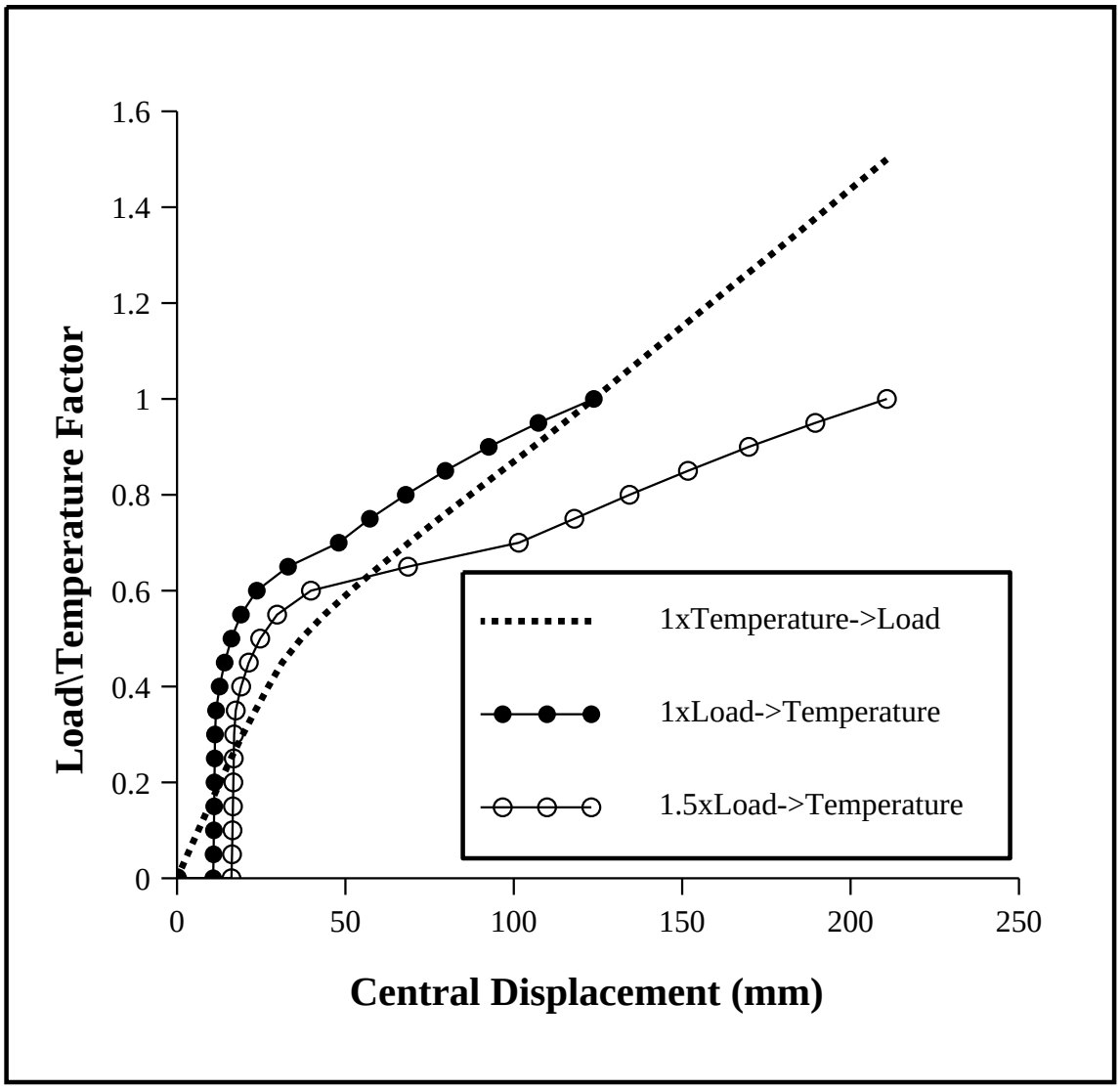

Figure 5.b. No thermal expansion: Refined model

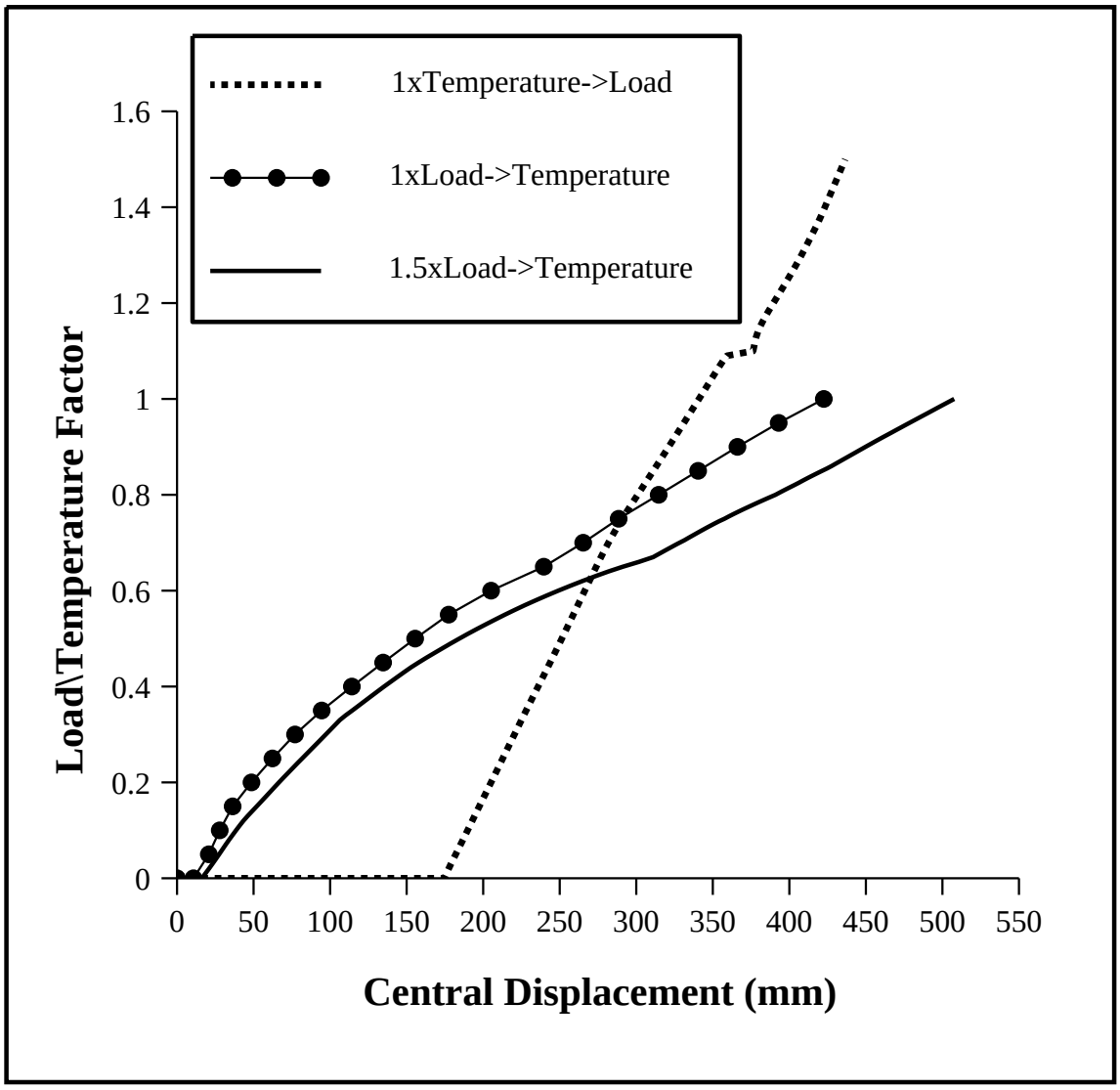

Figure 6.a. With thermal expansion: Refined model

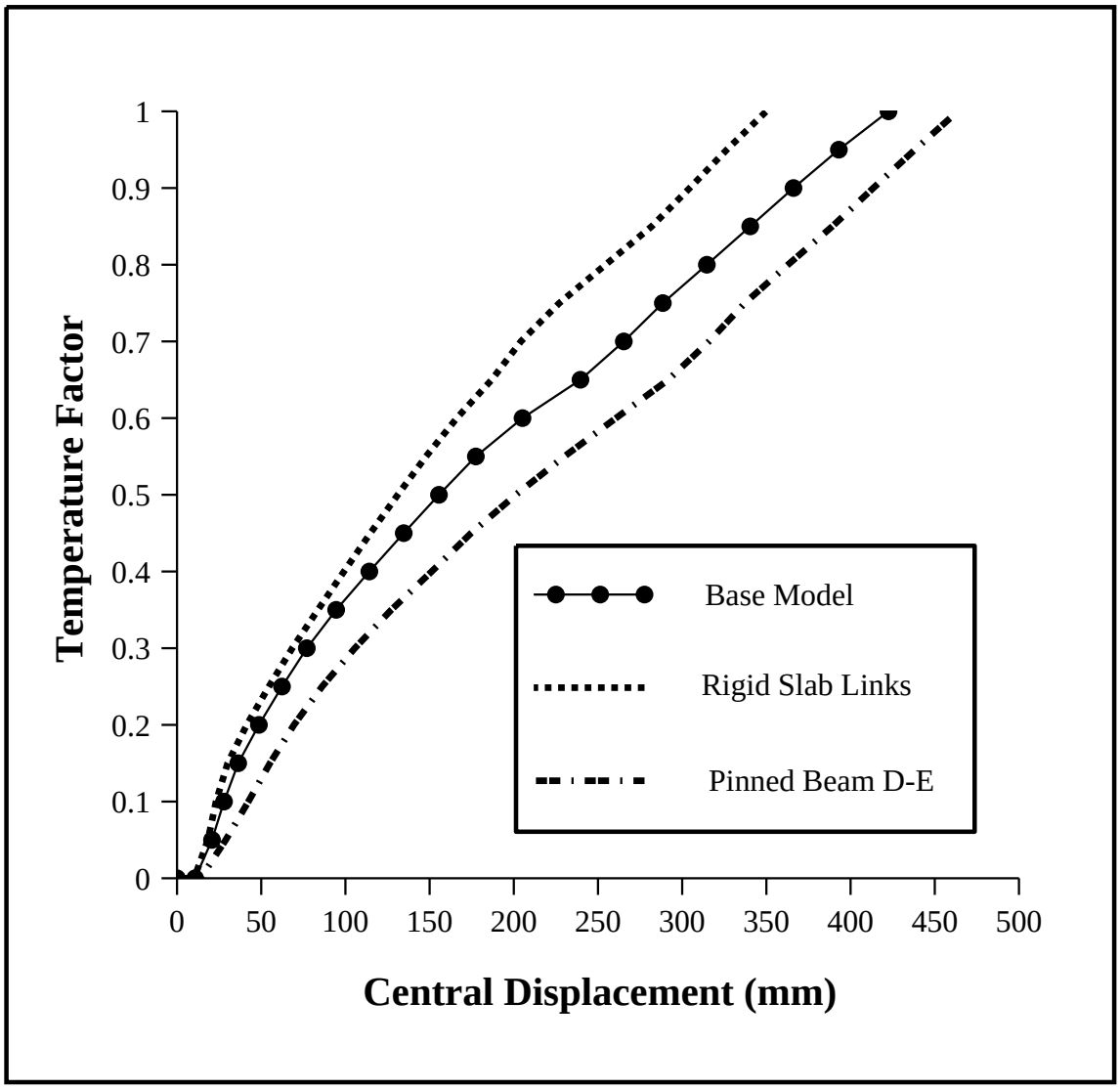

Figure 6.b. With thermal expansion: Effect of modelling assumptions

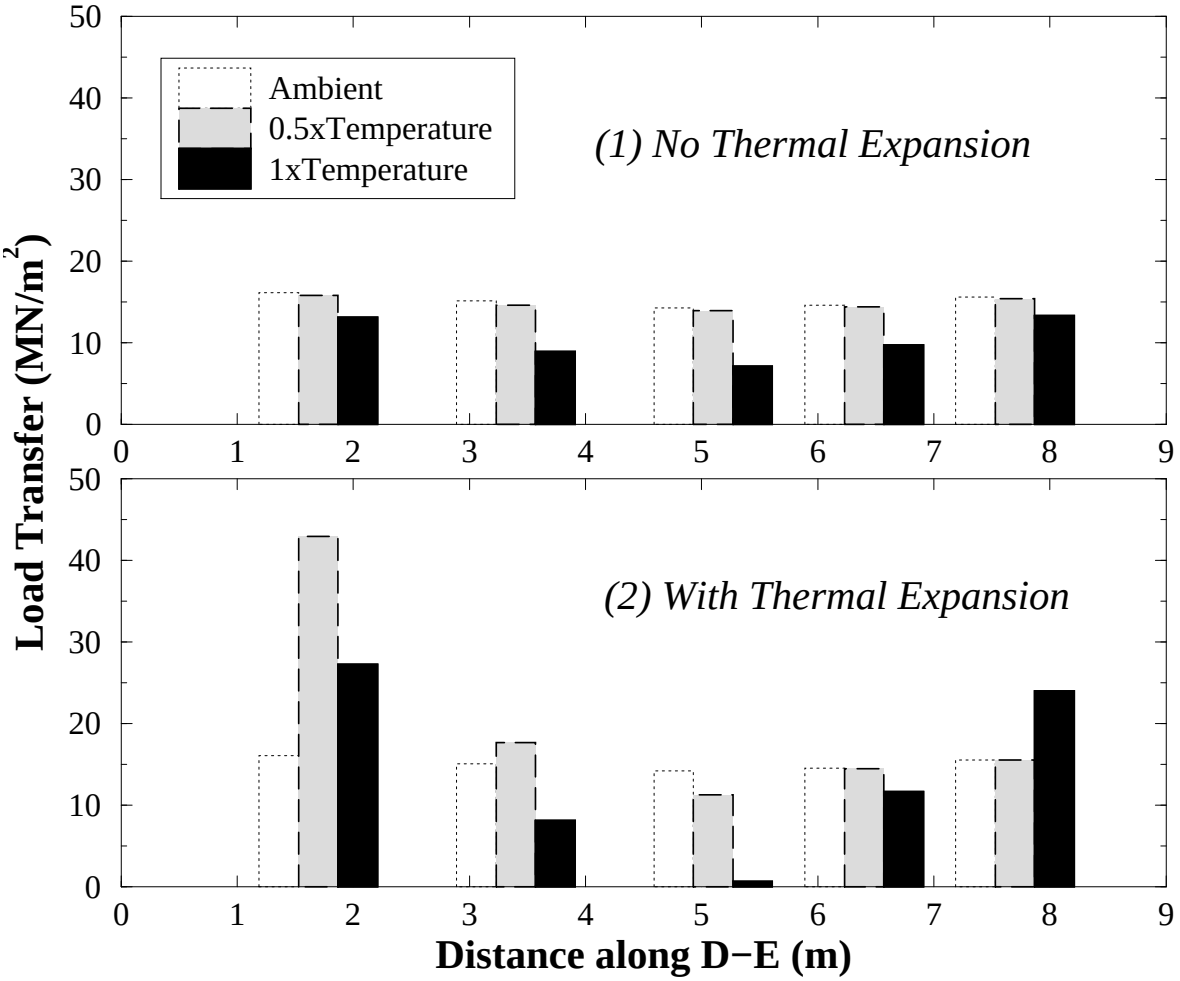

Figure 7. Load transfer between slab and composite beam D-E

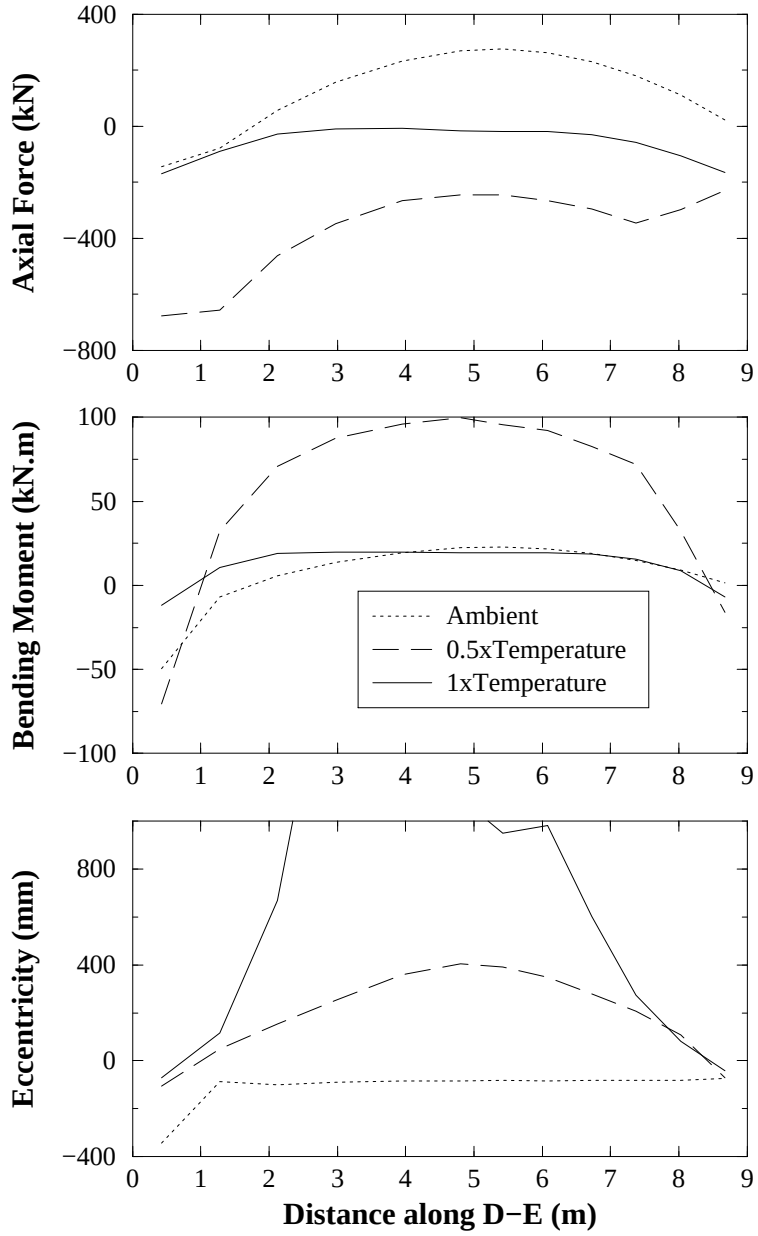

Figure 8. Axial force, bending moment and eccentricity in steel beam D-E

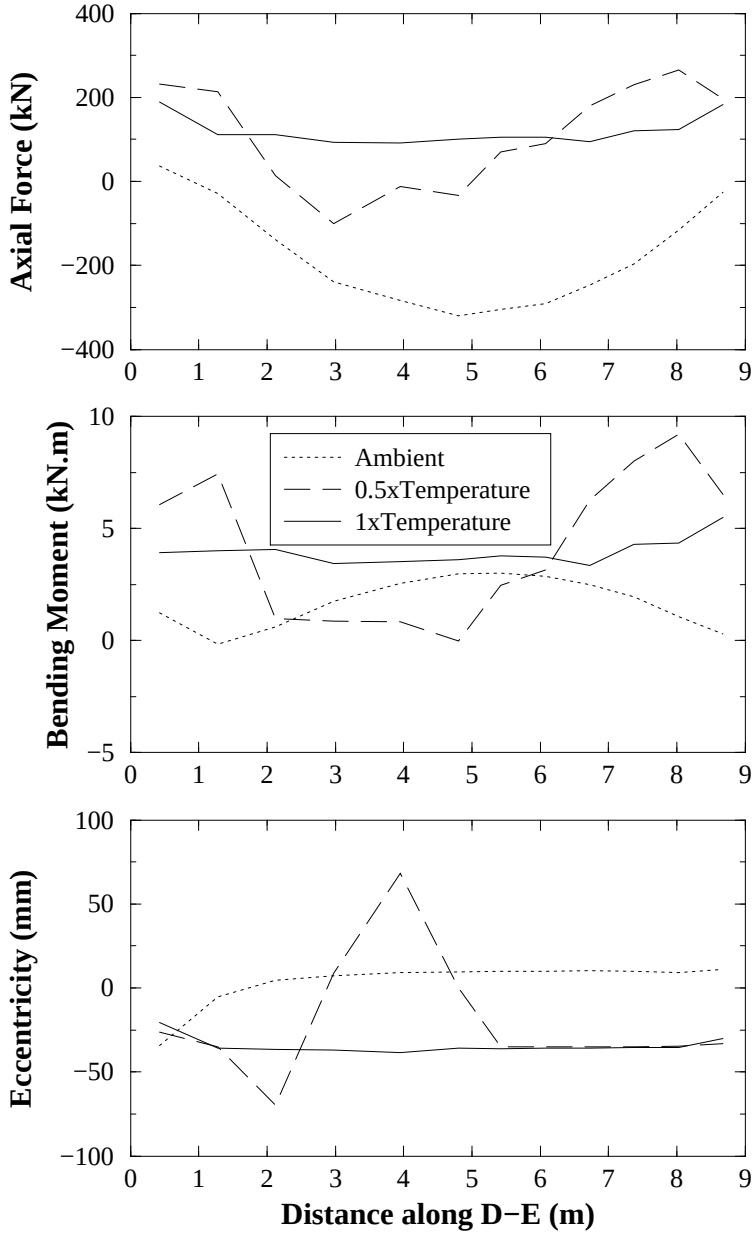

Figure 9. Axial force, bending moment and eccentricity in R/C rectangular beam D-E

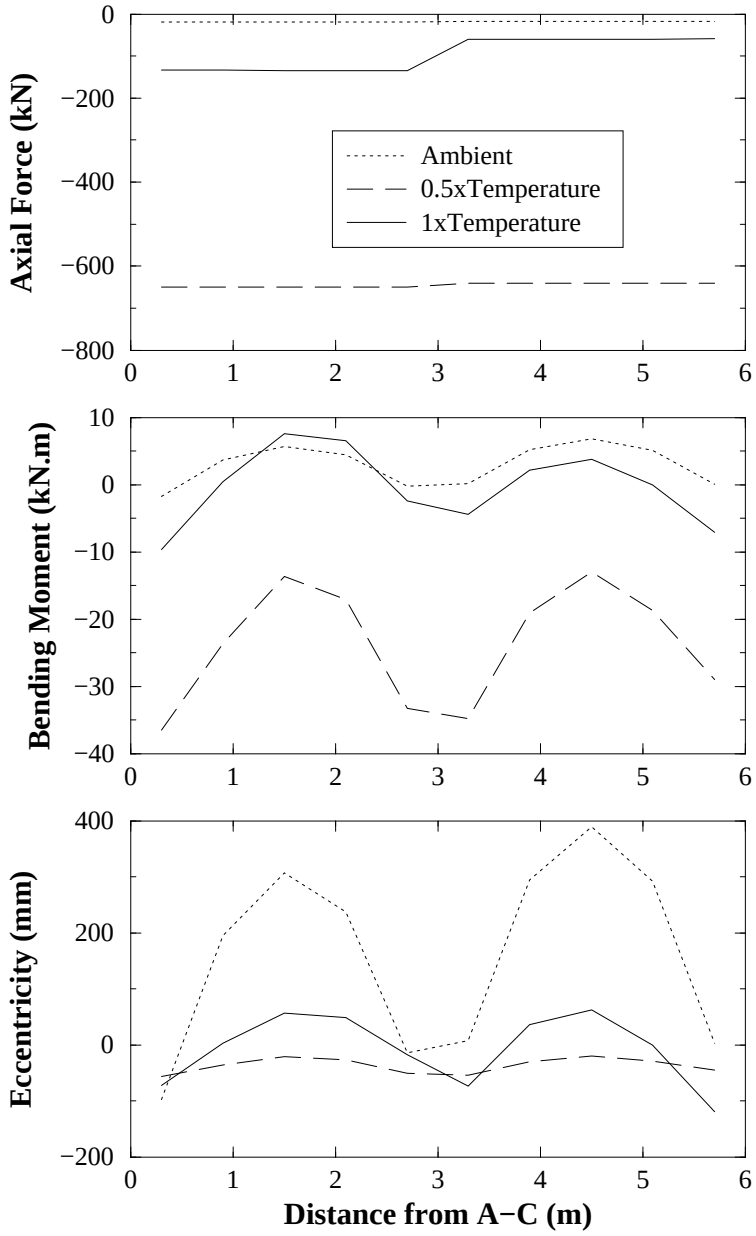

Figure 10. Axial force, bending moment and eccentricity in inner edge R/C T-beam

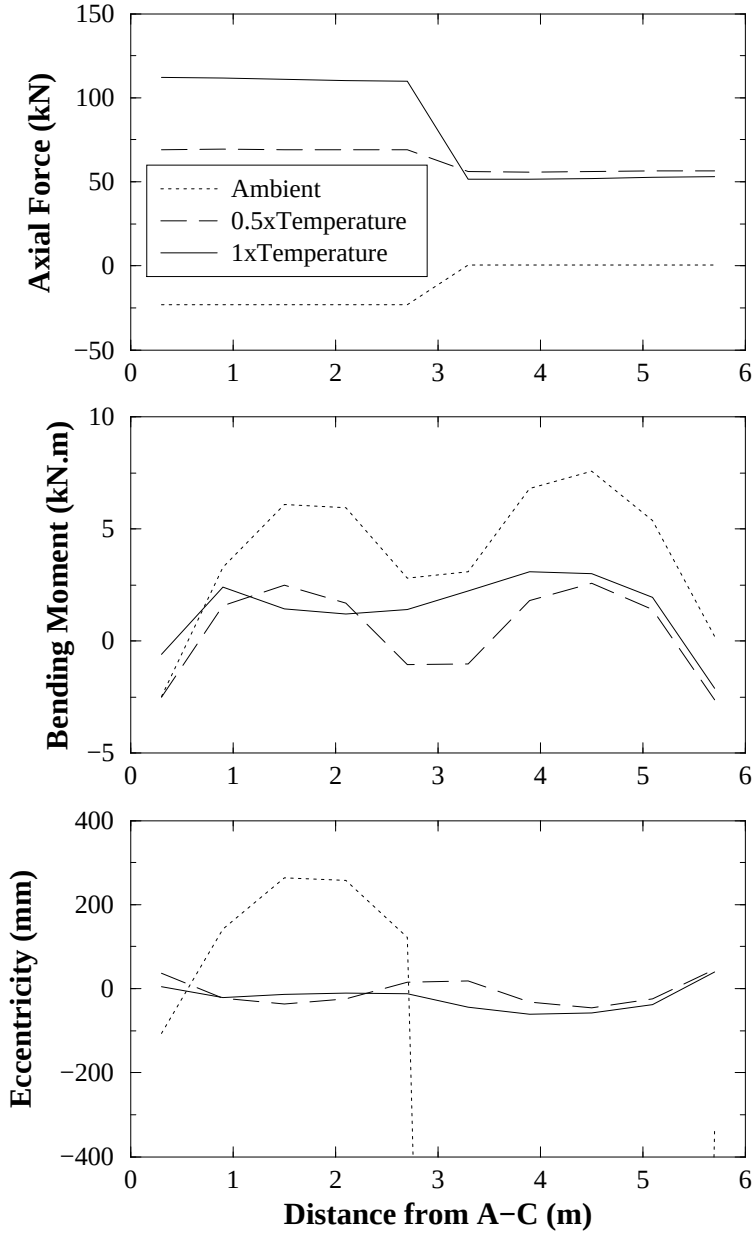

Figure 11. Axial force, bending moment and eccentricity in midspan R/C T-beam

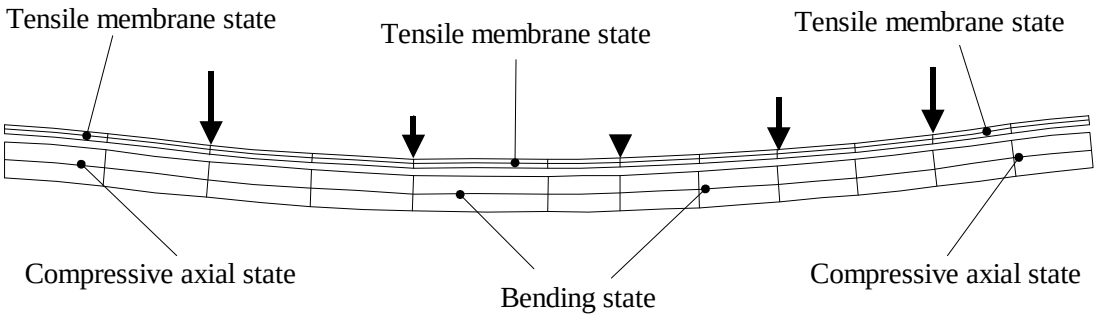

Figure 12. Composite beam D-E at full temperature

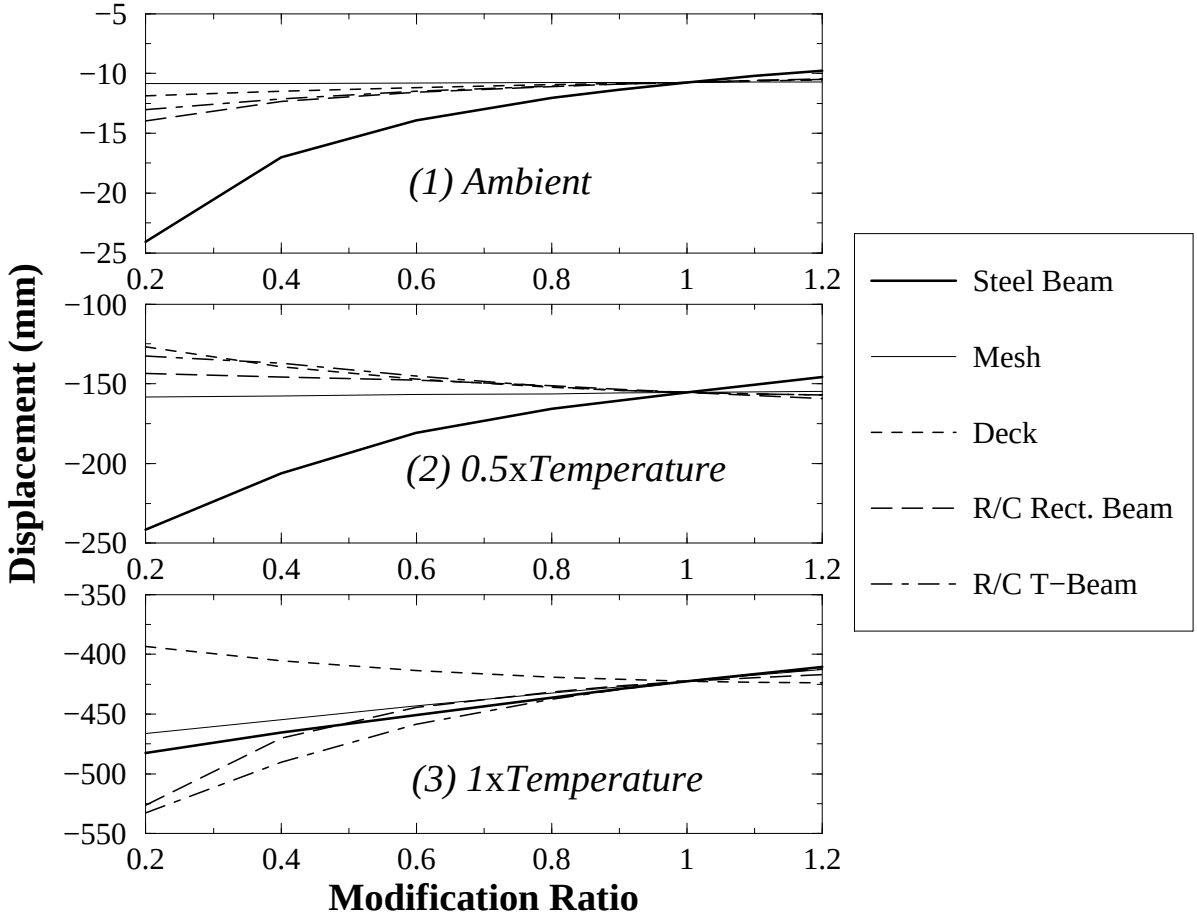

Figure 13.a. Effect of component sizes

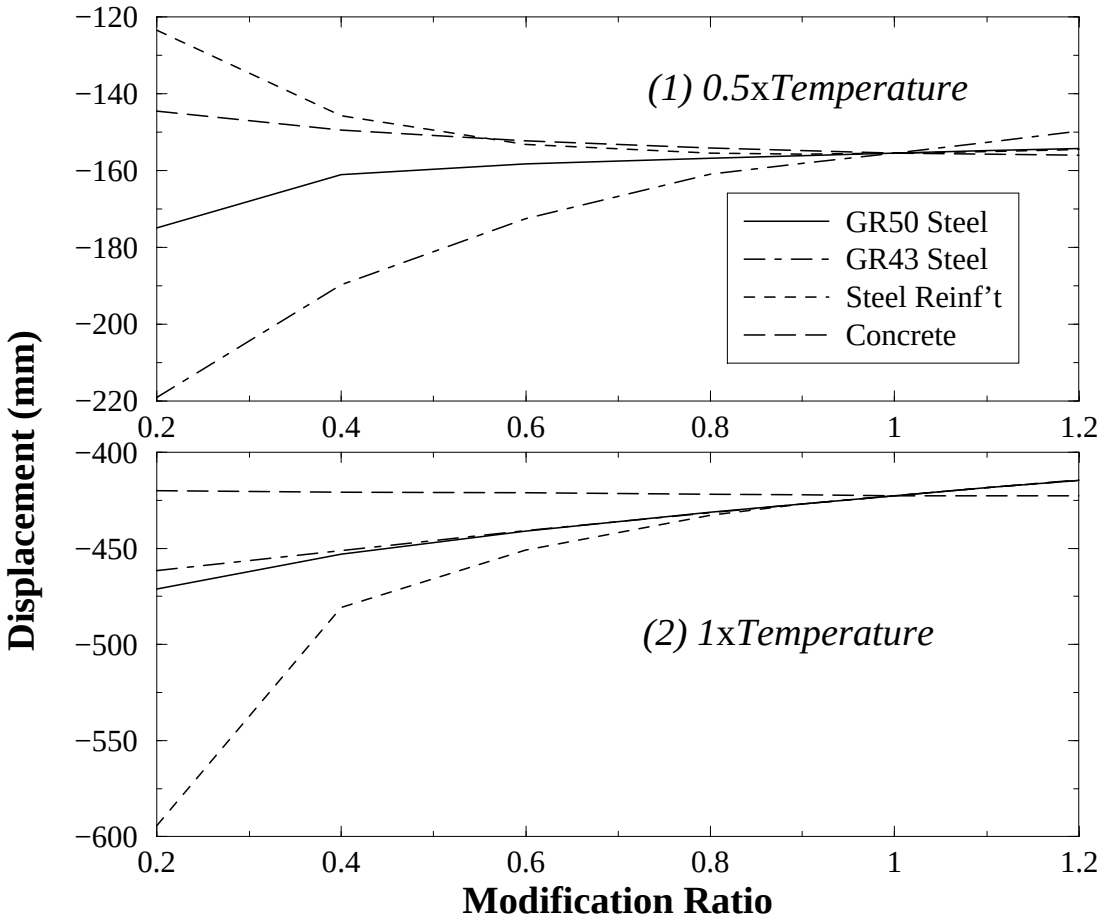

Figure 13.b. Effect of material strength